

## Structure and magnetic properties of Cu–Ni alloy nanoparticles prepared by rapid microwave combustion method

J. ARUL MARY<sup>1</sup>, A. MANIKANDAN<sup>1</sup>, L. JOHN KENNEDY<sup>2</sup>, M. BOUOUDINA<sup>3,4</sup>,  
R. SUNDARAM<sup>5</sup>, J. JUDITH VIJAYA<sup>1</sup>

1. Catalysis and Nanomaterials Research Laboratory, Department of Chemistry Loyola College, Chennai 600034, India;

2. Materials Division, School of Advanced Sciences, Vellore Institute of Technology (VIT) University,  
Chennai Campus, Chennai 600127, India;

3. Department of Physics, College of Science, University of Bahrain, PO Box 32038, Kingdom of Bahrain;

4. Nanotechnology Centre, University of Bahrain, PO Box 32038, Kingdom of Bahrain;

5. Department of Chemistry, Presidency College, Chennai 600005, India

Received 26 August 2013; accepted 7 January 2014

**Abstract:** Cu–Ni alloy nanoparticles were prepared by a microwave combustion method with the molar ratios of Cu<sup>2+</sup> to Ni<sup>2+</sup> as 3:7, 4:6, 5:5, 6:4 and 7:3. The as-prepared samples were characterized by XRD, HR-SEM, EDX and VSM. XRD and EDX analyses suggest the formation of pure alloy powders. The average crystallite sizes were found to be in the range of 21.56–33.25 nm. HR-SEM images show the clustered/agglomerated particle-like morphology structure. VSM results reveal that for low Ni content (Cu<sub>5</sub>Ni<sub>5</sub>, Cu<sub>6</sub>Ni<sub>4</sub> and Cu<sub>7</sub>Ni<sub>3</sub>), the system shows paramagnetic behaviors, whereas for high Ni content (Cu<sub>3</sub>Ni<sub>7</sub> and Cu<sub>4</sub>Ni<sub>6</sub>), it becomes ferromagnetic.

**Key words:** microwave combustion; nanoparticles; Cu–Ni alloys; magnetization property

### 1 Introduction

The preparation of nanostructures with controlled size, morphology and composition of the materials are of great interest, because of their unique physical and chemical properties. Also, nanomaterials are of vast scientific and technological importance, due to their more potential applications than bulk materials. Recently, bimetallic nanoalloys are mainly attractive, due to their unusual magnetic [1–4], electronic [1], biological [5] and catalytic properties [6], their size and pure elemental cluster. Alloy magnetic particles with size in the nanometer range exhibit features quite different from those of the corresponding bulk counterparts [7].

Among the various alloys, the copper–nickel (Cu–Ni) alloy nanoparticles show good catalytic properties that depend on the mole ratio of Cu to Ni of precursors. Copper–nickel alloys are widely studied because they possess good catalytic, electronic and magnetic properties. Also, they are widely used for

industry applications, due to their excellent resistance to corrosion, high inherent resistance to biofouling and good fabricability [8]. This is the case for Ni-based bimetallic particles containing copper, which exhibit better catalytic activity [9] and selectivity than monometallic nickel. It was found that the magnetic properties of Cu–Ni alloy nanostructures depend on the amount of Ni or the Ni-rich regions in the sample [10].

The copper–nickel alloys are known for the capable assembly of such materials. This well-considered alloy material is chemically stable and biocompatible and exhibits appropriate magnetic properties. Various techniques have been used to produce the bimetallic nanoalloys including the sol–gel [3], solvothermal [11], polyol process [12], sonochemical [13] and microemulsion method [14]. But the above methods are always high-energy consuming and require rather long reaction time, complex, low-yield and high cost.

In this present study, Cu–Ni bimetallic nanoalloys were synthesized by a microwave combustion method. However, microwave combustion method has more

advantages than the above methods, such as simple process, low cost and high purity products. Therefore, it is quite promising and easy to use for industrial applications. Recently, many oxide materials such as NiO nanoflakes,  $\text{Co}_3\text{O}_4$  nanocubes,  $\text{ZrO}_2$  nanospheres, MgO nanoflakes and Cu-doped  $\text{ZnFe}_2\text{O}_4$  nanoparticles, have also been prepared by a rapid microwave combustion method [15–17].

Due to the various applications of Cu–Ni bimetallic nanoalloys, many methods for the preparation of Cu–Ni alloys nanoparticles were used. Microwave combustion method has been rapidly developed and the obtained materials gained importance over the above methods. In this method, the microwaves interact with the reactants at the molecular level, as a result of rapid heating faster kinetics, homogeneity, higher yield, better reproducibility and energy saving [18]. This results in the formation of nanoparticles, early phase formation and different morphologies within few minutes [19]. The greatest advantage of microwave combustion is that it can heat a substance uniformly throughout a reaction container, leading to a more homogeneous nucleation and a shorter crystallization time compared with conventional combustion method [20].

Hence, in the present study, we prepared Cu–Ni alloys nanoparticles by a microwave combustion method and reported their structural, optical and magnetic properties. Then by changing the molar ratio of Cu to Ni, Cu–Ni alloy particles with different compositions were obtained. The products were characterized by X-ray diffraction (XRD), high resolution scanning electron microscopy (HR-SEM), energy dispersive X-ray analysis (EDX) and vibrating sample magnetometry (VSM) analysis.

## 2 Experimental

### 2.1 Material and method

All the chemicals used in this study were of analytical grade obtained from Merck, India, and were used as received without further purification. The samples were prepared with different mole ratios of Cu to Ni (3:7, 4:6, 5:5, 6:4 and 7:3). A stoichiometric ratio of  $\text{Cu}(\text{NO}_3)_2$ ,  $\text{Ni}(\text{NO}_3)_3$  and Triton X-100 (used as the reducing agent) were taken as precursors, which were stirred for 45 min, to get a clear homogeneous solution. In the case of mole ratio of Cu to Ni (5:5), the precursor mixture in Triton X-100 was placed in a domestic microwave oven and exposed to the microwave energy in a 2.45 GHz multimode cavity at 850 W for 10 min. Initially, the precursor mixture boiled and underwent evaporation followed by the decomposition with the evolution of gases. When the solution reached the point

of spontaneous combustion, it vaporized and instantly became a solid. Nitrogen gas was bubbled up continuously during the reaction, which created an inert atmosphere. The obtained samples were labeled as  $\text{Cu}_3\text{Ni}_7$ ,  $\text{Cu}_4\text{Ni}_6$ ,  $\text{Cu}_5\text{Ni}_5$ ,  $\text{Cu}_6\text{Ni}_4$  and  $\text{Cu}_7\text{Ni}_3$ , respectively.

### 2.2 Characterization

Structural characterizations of Cu–Ni (3:7, 4:6, 5:5, 6:4 and 7:3 in mole ratio) alloy nanoparticles were performed using a Rigaku Ultima IV high resolution X-ray diffractometer (XRD) with Cu  $K_\alpha$  radiation at  $\lambda=1.5418$  Å. Morphological studies and energy dispersive X-ray analysis have been performed by a Jeol JSM6360 high resolution scanning electron microscope (HR-SEM) equipped with electron dispersive X-ray (EDX) for elemental chemical analysis. Magnetic measurements were carried out at room temperature using a PMC MicroMag 3900 model vibrating sample magnetometer (VSM) equipped with 1 T magnet.

## 3 Results and discussion

### 3.1 X-ray diffraction analysis

The structural phases of Cu–Ni alloy nanoparticles were determined by the X-ray diffraction pattern. The XRD patterns of the as-synthesized Ni–Cu alloy nanoparticles with different compositions are shown in Fig. 1. The existence of strong and sharp diffraction peaks at  $2\theta$  located at  $43.51^\circ$ ,  $50.81^\circ$  and  $74.81^\circ$ , corresponding to (111), (200) and (220) planes, indicated the formation of a pure cubic Cu–Ni alloy nanoparticles [10]. This indicates that the precursors are completely converted into Cu–Ni alloy nanoparticles, which suggests the formation of a Cu–Ni solid solution of bimetallic nanoparticles. All the peaks correspond to Cu–Ni alloys with a face-centered cubic crystalline structure (JCPDS No. 09–0205).

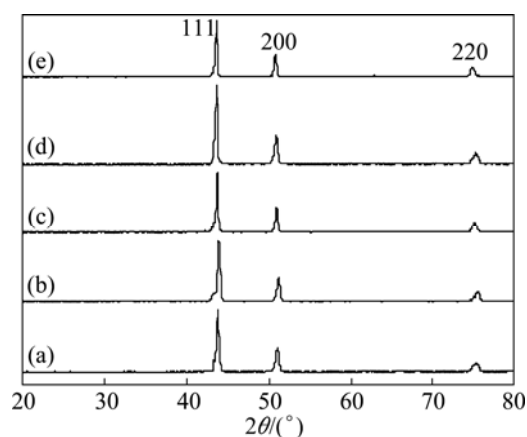


**Fig. 1** XRD patterns of  $\text{Cu}_3\text{Ni}_7$  (a),  $\text{Cu}_4\text{Ni}_6$  (b),  $\text{Cu}_5\text{Ni}_5$  (c),  $\text{Cu}_6\text{Ni}_4$  (d) and  $\text{Cu}_7\text{Ni}_3$  (e) samples

The XRD results reveal the straight forward formation of Cu–Ni alloys throughout the microwave combustion process in agreement with the complete solid solubility to form the Cu–Ni system. A progressive shift of the Bragg peaks to higher diffraction angles in both cases of (111) and (200) is observed as the Ni content increases. These results suggest the formation of the Cu–Ni solid solution by means of the diffusion of Cu through the Ni structure. Similar results were observed by BAN et al [21].

The average crystallite size was calculated using Scherrer's formula [15] given in Eq. (1).

$$L = \frac{0.89\lambda}{\beta \cos \theta} \quad (1)$$

where  $L$  is the crystallite size;  $\lambda$  is the X-ray wavelength;  $\theta$  is the Bragg diffraction angle;  $\beta$  is the full width at half maximum (FWHM). The average crystallite size  $L$  calculated from the diffraction peaks was found to be  $21.56^\circ$ – $33.25^\circ$  nm for Ni–Cu alloy nanoparticles. The estimated results show that the average crystallite size is higher (33.25 nm) for  $\text{Cu}_3\text{Ni}_7$  sample, while the crystallite size is decreased to 21.56 nm for the  $\text{Cu}_7\text{Ni}_3$  sample (Fig. 2). The results reveal that the crystallite size decreases with increasing the Ni content, thus confining to the smaller dimension.

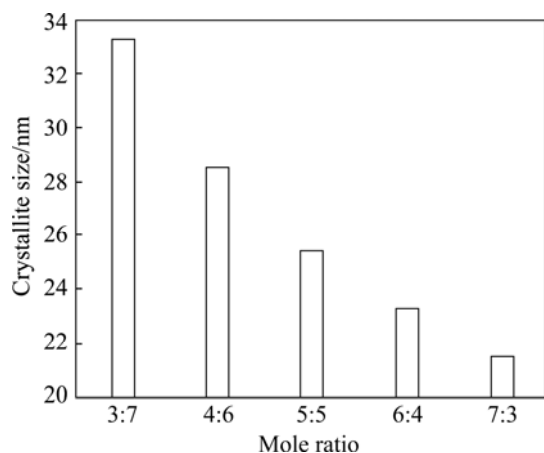


**Fig. 2** Crystallite size of Cu–Ni alloy nanoparticles with different mole ratios of Cu to Ni

The lattice parameters were calculated using the formula given in Eq. (2) [22].

$$\sin^2 \theta = \frac{\lambda^2}{4} \left[ \frac{4}{3} \left( \frac{h^2 + hk + k^2}{a^2} \right) + \frac{l^2}{c^2} \right] \quad (2)$$

where  $\theta$  is the diffraction angle;  $\lambda$  is the incident wavelength ( $\lambda=1.540$  Å);  $h$ ,  $k$ , and  $l$  are Miller's indices. The lattice parameters of Cu–Ni alloys are found to be 3.554, 3.562, 3.569, 3.578, and 3.588 Å for  $\text{Cu}_3\text{Ni}_7$ ,  $\text{Cu}_4\text{Ni}_6$ ,  $\text{Cu}_5\text{Ni}_5$ ,  $\text{Cu}_6\text{Ni}_4$  and  $\text{Cu}_7\text{Ni}_3$ , respectively

(Fig. 3). The value increases with decreasing the Ni content. Because the atomic radius of Cu (1.278 Å) is larger than that of Ni (1.246 Å), the lattice parameter of high-Cu region will be larger than that of low-Cu region. This coexistence of high-Cu and low-Cu regions in the Cu–Ni alloy nanoparticles will be further confirmed by EDX. The calculated lattice parameters are very close to the reported values of bulk Ni (3.525 Å, ICSD No. 44767) and bulk Cu (3.615 Å, ICSD No. 64699) [10]. The phase diagram of Cu–Ni binary system [23] shows that a substitutional solid solution forms as both Cu and Ni crystallize in the face centered cubic structure.

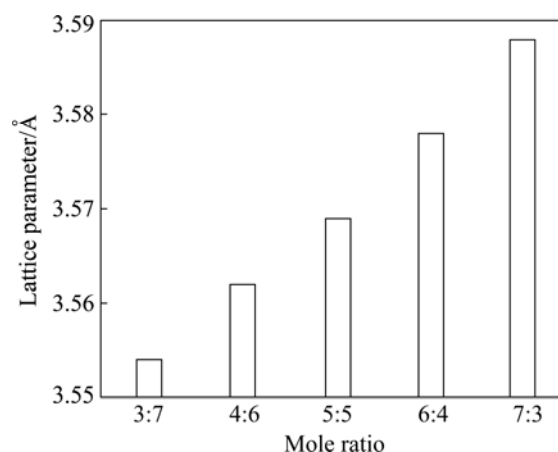


**Fig. 3** Lattice parameters of Cu–Ni alloy nanoparticles with different mole ratios of Cu to Ni

### 3.2 SEM analysis

The morphological characteristics of the obtained Cu–Ni alloy nanoparticles were investigated by high resolution scanning electron microscope (HR-SEM) as shown in Fig. 4. Figure 4 shows the particle-like morphology with a strong agglomeration, due to the magnetic characteristics of the samples [24]. Figures 4(a) and (b) show the HR-SEM images of  $\text{Cu}_3\text{Ni}_7$  alloy nanoparticles and the average particle size is 36 nm. Figures 4(c) and (d) show the HR-SEM images of  $\text{Cu}_5\text{Ni}_5$  alloy nanoparticles and the average particle size is 27 nm. Figures 4(e) and (f) show the HR-SEM images of  $\text{Cu}_7\text{Ni}_3$  alloy nanoparticles and the average particle size is 23 nm. These values are in good agreement with the XRD analysis results.

Therefore, we can infer that the agglomerated Cu–Ni crystals are formed during the combustion process. In this approach, microwave oven operated at a power of 850 W (2.45 GHz) produced enormous amount of heat and made the sudden combustion process form nano-sized particles. Therefore, it is clearly understood that in the microwave method, during microwave combustion, the molecular dipoles are induced to oscillate by the microwave. This oscillation causes higher rates of molecular collision, which generates

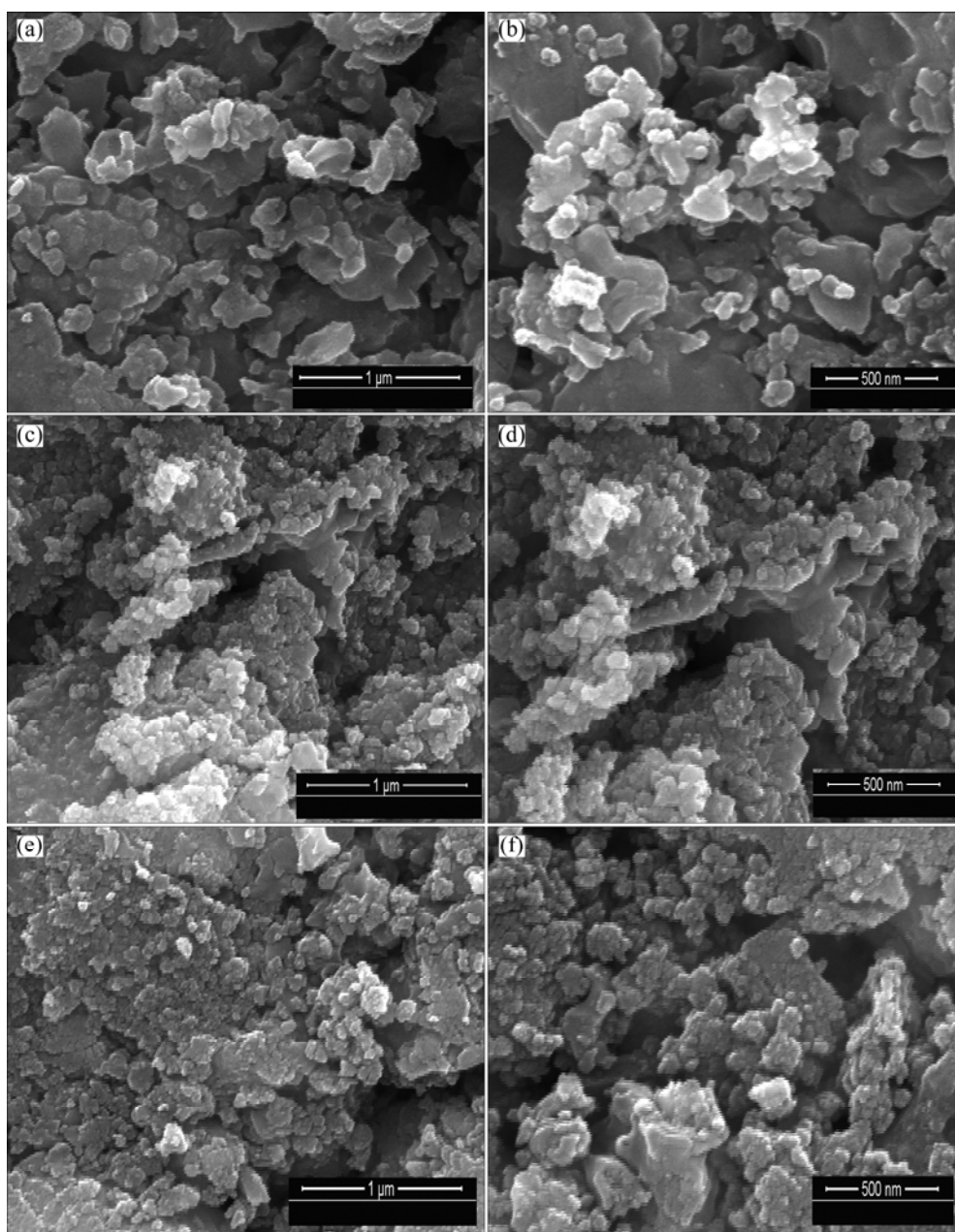


**Fig. 4** HR-SEM images of  $\text{Cu}_3\text{Ni}_7$  (a,b),  $\text{Cu}_5\text{Ni}_5$  (c,d) and  $\text{Cu}_7\text{Ni}_3$  (e,f) samples

enormous amount of heat, consequently the temperature distribution is homogeneous and transferred to the materials interior, making the explosion reaction followed by vigorous evolution of gases form nanoparticles-like morphology.

### 3.3 EDX analysis

The composition of Cu–Ni alloy nanoparticles was analyzed by energy dispersive X-ray analysis (EDX), as shown in Fig. 5. The EDX results show the presence of Ni and Cu by the appearance of Ni and Cu peaks without any other characteristic peaks. Hence, the results are definitive evidence to suggest that the Cu–Ni alloy nanoparticles do not contain any other elements and are

indeed free from other impurities. The compositions of the Cu–Ni nanoparticles are consistent with the mole ratios of  $\text{Cu}^{2+}$  to  $\text{Ni}^{2+}$  used for the synthesis (inset in Fig. 5).

### 3.4 VSM measurements

The magnetic hysteresis ( $M-H$ ) of the Cu–Ni alloy nanoparticles is shown in Fig. 6. It was recorded using a vibrating sample magnetometer (VSM) in the applied field range from  $-795.78$  to  $795.78$  kA/m at room temperature. Cu–Ni alloy nanoparticles are important magnetic materials, and many efforts have been made to control the size of nanoparticles, because of their particle size depending on the magnetic properties. VSM

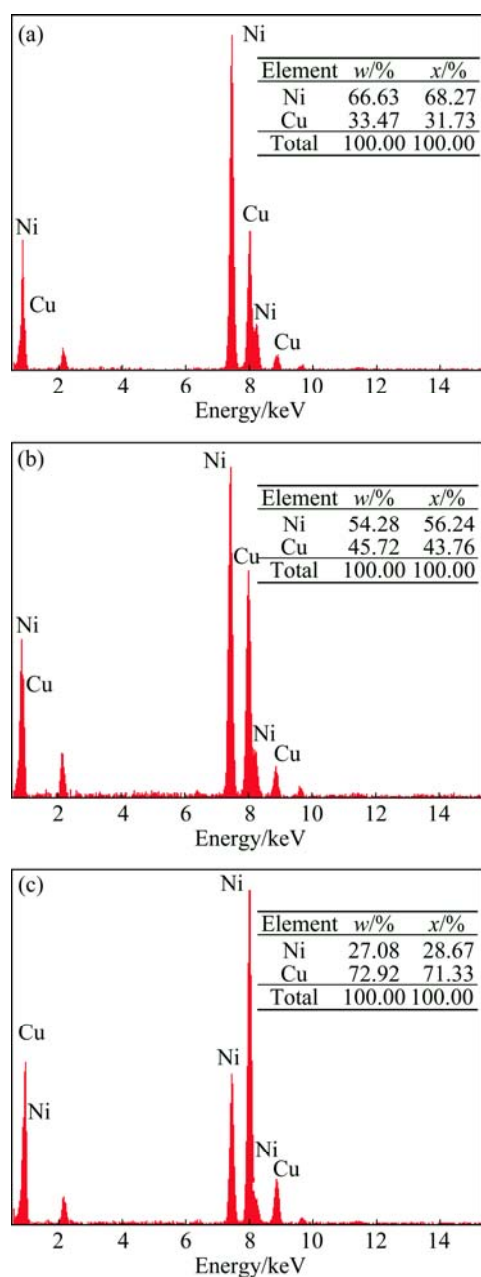


**Fig. 5** EDX spectra of Cu<sub>3</sub>Ni<sub>7</sub> (a), Cu<sub>5</sub>Ni<sub>5</sub> (b) and Cu<sub>7</sub>Ni<sub>3</sub> (c) samples

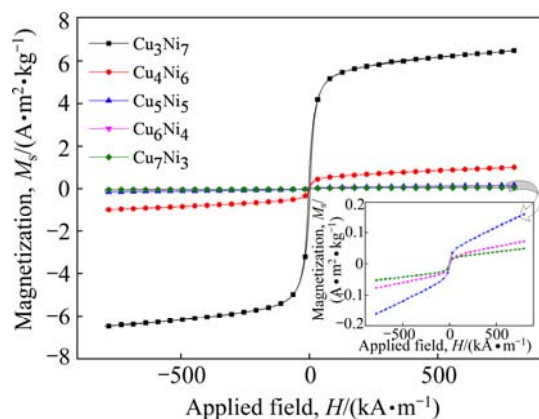


**Fig. 6** Magnetic hysteresis ( $M$ - $H$ ) loops of Cu-Ni alloy nanoparticles with different mole ratios of 3:7, 4:6, 5:5, 6:4 and 7:3

measurements were carried out on the as-synthesized Cu-Ni alloy nanoparticles. The variations of coercivity ( $H_c$ ), remnant magnetization ( $M_r$ ) and saturation magnetization ( $M_s$ ) of the obtained Cu-Ni alloy nanoparticles are shown in Fig. 7 and Table 1. It was found that the saturation and remnant magnetization increase with the increase in Ni content of the Cu-Ni alloys [24]. The magnetization of Cu<sub>3</sub>Ni<sub>7</sub> and Cu<sub>4</sub>Ni<sub>6</sub> samples shows ferromagnetic behavior and Cu<sub>5</sub>Ni<sub>5</sub>, Cu<sub>6</sub>Ni<sub>4</sub> and Cu<sub>7</sub>Ni<sub>3</sub> samples are super paramagnetic. But copper is diamagnetic [22] and nickel is ferromagnetic in nature [25]. Similar values are reported by YAMAUCHI et al [26].

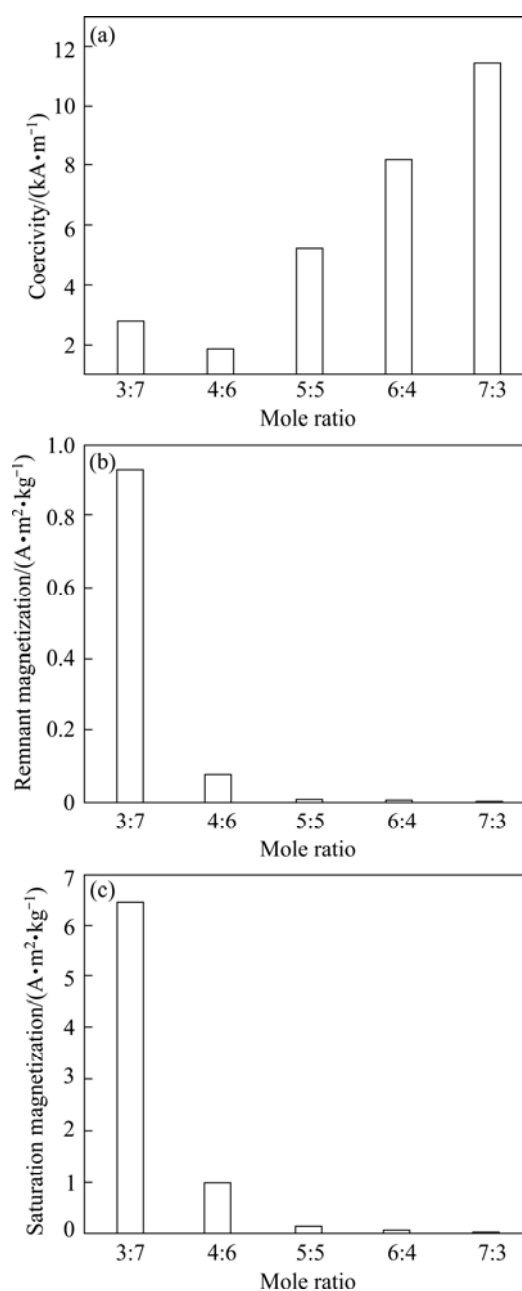


**Fig. 7** VSM results of Cu-Ni alloy nanoparticles with different mole ratios of Cu to Ni: (a) Coercivity; (b) Remnant magnetization; (c) Saturation magnetization

**Table 1** Lattice parameter, crystallite size and magnetic properties of Ni–Cu alloy nanoparticles

Sample	Lattice parameter/ Å	Crystallite size/ nm	$H_c$ / (A·m <sup>-1</sup> )	$M_r$ / (A·m <sup>2</sup> ·kg <sup>-1</sup> )	$M_s$ / (A·m <sup>2</sup> ·kg <sup>-1</sup> )
Cu <sub>3</sub> Ni <sub>7</sub>	3.554	33.25	2790.60	0.937	6.478
Cu <sub>4</sub> Ni <sub>6</sub>	3.562	28.54	1856.68	0.076	0.997
Cu <sub>5</sub> Ni <sub>5</sub>	3.569	25.49	5200.64	0.009	0.161
Cu <sub>6</sub> Ni <sub>4</sub>	3.578	23.37	8184.72	0.005	0.073
Cu <sub>7</sub> Ni <sub>3</sub>	3.588	21.56	11472.99	0.004	0.049

The magnetic hysteresis ( $M$ – $H$ ) loops of the Cu<sub>5</sub>Ni<sub>5</sub>, Cu<sub>6</sub>Ni<sub>4</sub> and Cu<sub>7</sub>Ni<sub>3</sub> alloy powders show very low remnant magnetization at room temperature, indicating the super paramagnetic behavior of the Cu–Ni nanoparticles. The coercivity increases with decreasing the Ni content. The saturation magnetization of the samples is between 0.049 and 6.478 A·m<sup>2</sup>/kg and depends on the concentration of nickel in the prepared alloy samples [27]. However, as the copper content increases in these nanocrystalline alloys, the magnetization is decreased [21]. The bimetallic nanoparticles Cu<sub>3</sub>Ni<sub>7</sub> and Cu<sub>4</sub>Ni<sub>6</sub> show the ferromagnetic behavior and the magnetization decreases with increase in content of copper (Cu<sub>5</sub>Ni<sub>5</sub>, Cu<sub>6</sub>Ni<sub>4</sub> and Cu<sub>7</sub>Ni<sub>3</sub>). The dependence of saturation magnetization on the Ni content of the Cu–Ni alloys has also been reported by BASKARAN et al [27].

## 4 Conclusions

The Cu–Ni alloy nanoparticles were successfully prepared by a simple microwave combustion method with the mole ratios of Cu<sup>2+</sup> to Ni<sup>2+</sup> of 3:7, 4:6, 5:5, 6:4 and 7:3. The XRD results of Cu–Ni alloy nanoparticles reveal that the crystalline phase maintains the cubic structure for all the compositions. The lattice parameter decreases with the increase in the Ni content of the Cu–Ni alloy, i.e. 8.588 to 8.554 Å, due to the smaller atomic radius of Ni (1.246 Å) than Cu (1.278 Å). The average crystallite size of the samples reveals that the increase in Ni content leads to increasing the crystallite size from 21.56 to 33.25 nm, which ultimately affects the magnetic properties. The magnetization of Cu<sub>3</sub>Ni<sub>7</sub> and Cu<sub>4</sub>Ni<sub>6</sub> samples shows ferromagnetic properties with higher saturation magnetization than Cu<sub>5</sub>Ni<sub>5</sub>, Cu<sub>6</sub>Ni<sub>4</sub> and Cu<sub>7</sub>Ni<sub>3</sub> samples. The saturation magnetization increases with the increase in Ni content of the Cu–Ni alloys.

## References

[1] JO C, LEE J I, JANG Y. Electronic and magnetic properties of

ultrathin Fe–Co alloy nanowires [J]. Chemistry of Materials, 2005, 17: 2667–2671.

[2] SINGH P P. Relativity and magnetism in Ni–Pd and Ni–Pt alloys [J]. Journal of Magnetism and Magnetic Materials, 2003, 26: 347–352.

[3] MATTEI G, de FERNANDEZ JULIAN C, MAZZOLDI P, SADA C, DE G, BATTAGLIN G, SANGREGORIO C, GATTESCHI D. Synthesis, structure, and magnetic properties of Co, Ni, and Co–Ni alloy nanocluster-doped SiO<sub>2</sub> films by sol-gel processing [J]. Chemistry of Materials, 2002, 14: 3440–3447.

[4] HAN S W, KIM Y, KIM K. Dodecanethiol-derivatized Au/Ag bimetallic nanoparticles: TEM, UV/VIS, XPS, and FTIR analysis [J]. Journal of Colloid and Interface Science, 1998, 208(1): 272–278.

[5] HONG R, FISCHER N O, EMRICK T, ROTELLO V M. Surface PEGylation and ligand exchange chemistry of FePt nanoparticles for biological applications [J]. Chemistry of Materials, 2005, 17(18): 4617–4621.

[6] ZHANG X, CHAN K Y. Water-in-oil microemulsion synthesis of platinum-ruthenium nanoparticles, their characterization and electrocatalytic properties [J]. Chemistry of Materials, 2003, 15(2): 451–459.

[7] HIMPEL F J, ORTEGA J E, MANKEY G J, WILLIS R F. Magnetic nanostructures [J]. Advances in Physics, 1998, 47: 511–597.

[8] FANG T H, WU C D, CHANG W J, CHI S S. Effect of thermal annealing on nanoimprinted Cu–Ni alloys using molecular dynamics simulation [J]. Applied Surface Science, 2009, 255: 6043–6047.

[9] LI Y, CHEN J, CHANG L, QIN Y. The doping effect of copper on the catalytic growth of carbon fibers from methane over a Ni/Al<sub>2</sub>O<sub>3</sub> catalyst prepared from Feitknecht compound precursor [J]. Journal of Catalysis, 1998, 178: 76–83.

[10] MO Guang, CHENG Wei-dong, CAI Quan, WANG Wei, ZHANG Kun-hao, XING Xue-qing, CHEN Zhong-jun, WU Zhong-hua. Structural change of Ni–Cu alloy nanowires with temperature studied by in situ X-ray absorption fine structure technique [J]. Materials Chemistry and Physics, 2010, 121: 390–394.

[11] WANG Wei-hua, CAO Geng-yu. Synthesis and structural investigation of Pd/Ag bimetallic nanoparticles prepared by the solvothermal method [J]. Journal of Nanoparticle Research, 2007, 9: 1153–1161.

[12] LIU C, WU X, KLEMMER T, SHUKLA N, WELLER D, ROY A G, TANASE M, LAUGHLIN D. Reduction of sintering during annealing of FePt nanoparticles coated with iron oxide [J]. Chemistry of Materials, 2005, 17: 620–625.

[13] SHAFI K, GEDANKEN A, GOLDFARB R B, FELNER I. Sonochemical preparation of nanosized amorphous Fe–Ni alloys [J]. Journal of Applied Physics, 1997, 81: 6901–6905.

[14] WEN Ming, LIU Qiu-yan, WANG Ya-fen, ZHU Yuan-zheng, WU Qing-sheng. Positive microemulsion synthesis and magnetic property of amorphous multicomponent Co-, Ni- and Cu-based alloy nanoparticles [J]. Colloids and Surfaces A: Physicochemical and Engineering Aspects, 2008, 318: 238–244.

[15] MANIKANDAN A, JUDITH VIJAYA J, JOHN KENNEDY L. Comparative investigation of NiO nano- and microstructures for structural, optical and magnetic properties [J]. Physica E, 2013, 49: 117–123.

[16] SELVAM N C S, MANIKANDAN A, JOHN KENNEDY L, JUDITH VIJAYA J. Comparative investigation of zirconium oxide (ZrO<sub>2</sub>) nano and microstructures for structural, optical and photocatalytic properties [J]. Journal of Colloid and Interface Science, 2013, 389: 91–98.

[17] MANIKANDAN A, VIJAYA J J, KENNEDY L J, BOUOUDINA M. Structural, optical and magnetic properties of Zn<sub>1-x</sub>Cu<sub>x</sub>Fe<sub>2</sub>O<sub>4</sub> nanoparticles prepared by microwave combustion method [J]. Journal of Molecular Structure, 2013, 1035: 332–340.

- [18] NI H, NI Y H, ZHOU Y Y, HONG J M. Microwave–hydrothermal synthesis, characterization and properties of rice-like  $\alpha$ -Fe<sub>2</sub>O<sub>3</sub> nanorods [J]. Materials Letters, 2012, 73: 206–208.
- [19] MANGALARAJA R V, MOUZON J, HEDSTROM P, CAMURRI C P, ANANTHAKUMAR S, ODEN M. Microwave assisted combustion synthesis of nanocrystalline yttria and its powder characteristics [J]. Powder Technology, 2009, 191: 309–314.
- [20] KIJIMA N, YOSHINAGA M, AWAKA J, AKIMOTO J. Microwave synthesis, characterization, and electrochemical properties of  $\alpha$ -Fe<sub>2</sub>O<sub>3</sub> nanoparticles [J]. Solid State Ionics, 2011, 192: 293–297.
- [21] BAN I, STERGAR J, DROFENIK M, FERK G, MAKOVEC D. Synthesis of copper-nickel nanoparticles prepared by mechanical milling for use in magnetic hyperthermia [J]. Journal of Magnetism and Magnetic Materials, 2011, 323: 2254–2258.
- [22] JILES D. Introduction to magnetism and magnetic materials [M]. 1st edition. London: Chapman Hall, 1991.
- [23] MASSALSKI T B. Binary alloy phase diagrams [M]. 2nd edition. Materials Park, Ohio: ASM International, 1990: 1442.
- [24] GIMENES R, BALDISSERA M R, da SILVA M R A, da SILVA M R, ZAGHETE M A. Structural and magnetic characterization of Mn<sub>x</sub>Zn<sub>1-x</sub>Fe<sub>2</sub>O<sub>4</sub> (x=0.2; 0.35; 0.65; 0.8; 1.0) ferrites obtained by the citrate precursor method [J]. Ceramics International, 2012, 38: 741–746.
- [25] HANDLEY R C. Modern magnetic materials [M]. New York: Wiley, 2000.
- [26] YAMAUCHI T, TSUKAHARA Y, SAKATA T, MORI H, YANAGIDA T, KAWAI T, WADA Y. Magnetic Cu–Ni (core–shell) nanoparticles in a one-pot reaction under microwave irradiation [J]. Nanoscale, 2010, 2: 515–523.
- [27] BASKARAN I, SANKARA NARAYANAN T S N, STEPHEN A. Pulsed electro-deposition of nanocrystalline Cu–Ni alloy films and evaluation of their characteristic properties [J]. Materials Letters, 2006, 60: 1990–1995.

## 快速微波燃烧法制备的 Cu–Ni 合金 纳米粒子结构和磁性能

J. ARUL MARY<sup>1</sup>, A. MANIKANDAN<sup>1</sup>, L. JOHN KENNEDY<sup>2</sup>, M. BOUOUDINA<sup>3,4</sup>,  
R. SUNDARAM<sup>5</sup>, J. JUDITH VIJAYA<sup>1</sup>

1. Catalysis and Nanomaterials Research Laboratory, Department of Chemistry Loyola College, Chennai 600034, India;

2. Materials Division, School of Advanced Sciences, Vellore Institute of Technology (VIT) University,  
Chennai Campus, Chennai 600127, India;

3. Department of Physics, College of Science, University of Bahrain, PO Box 32038, Kingdom of Bahrain;

4. Nanotechnology Centre, University of Bahrain, PO Box 32038, Kingdom of Bahrain;

5. Department of Chemistry, Presidency College, Chennai 600005, India

**摘 要:** 采用微波燃烧法制备 Cu<sup>2+</sup> 和 Ni<sup>2+</sup> 摩尔比分别为 3:7, 4:6, 5:5, 6:4 和 7:3 的 Cu–Ni 合金纳米粒子, 采用 XRD、HR-SEM、EDX 和 VSM 对所制备的样品进行表征。X 射线衍射和能谱分析表明, 在样品制备过程中形成了纯合金粉末。样品的平均晶粒尺寸为 21.56–33.25 nm。HR-SEM 像显示样品具有集群/团簇粒状形态结构。VSM 分析结果表明, 对于低 Ni 含量的合金(Cu<sub>5</sub>Ni<sub>5</sub>, Cu<sub>6</sub>Ni<sub>4</sub> 和 Cu<sub>7</sub>Ni<sub>3</sub>), 样品显示顺磁性, 而对于较高 Ni 含量的合金(Cu<sub>3</sub>Ni<sub>7</sub> 和 Cu<sub>4</sub>Ni<sub>6</sub>), 样品呈现铁磁性。

**关键词:** 微波燃烧; 纳米粒子; Cu–Ni 合金; 磁性能

(Edited by Xiang-qun LI)